14th Czech and Slovak Conference on Magnetism, Košice, Slovakia, July 6–9, 2010

Influence of Zn on Structure and Magnetic Properties of Rapid Quenched (Fe–Zn)–Cu–Nb–Si–B Alloys

V. Kolesar[a], S. Michalik[a], J. Kovac[b], V. Girman[a], P. Sovak[a] and P. Kollar[a]

[a]Institute of Physics, P.J. Safarik University, Park Angelinum 9, 041 54 Kosice, Slovakia

[b]Institute of Experimental Physics, Slovak Academy of Science, Watsonova 47, 041 01 Kosice, Slovakia

The aim of this work was to study the influence of Zn on the formation of nanostructure in $Fe_{73.5-x}Zn_xCu_1Nb_3Si_{13.5}B_9$ (x = 1, 3, 5) ribbons prepared by the melt-spinning technique. X-ray diffraction measurements proved amorphous state of the sample with $x = 1$. The sample with $x = 3$ contains a small fraction of Fe_3Si phase and the sample with $x = 5$ is in nanocrystalline state with the average grain size of about 25 nm. The reduced radial distribution function $G(r)$ was calculated for local structure investigation. Increasing Zn content enhances crystallization during solidification which leads to increase of magnetocrystalline anisotropy and consequently to increase of coercivity.

PACS numbers: 61.46.Hk, 75.50.Bb, 75.75.Cd

1. Introduction

Nanocrystalline Fe–Cu–Nb–Si–B alloy prepared from amorphous state by annealing at about 550 °C has excellent magnetic properties and a lot of potential applications such as magnetic parts of power transfers, magnetic sensors, actuators etc. [1–3]. Manufacturing of this alloy consists of two steps, i.e., formation of amorphous precursor by rapid solidification followed by well defined annealing which leads to formation of nanocrystalline phase [4, 5]. Annealing is energetically difficult process and production of nanocrystalline ribbons directly by the melt-spinning technique would be much advantageous. It was shown that the addition of Zn to the $Fe_{73.5}Si_{13.5}B_9Nb_3Cu_{1-x}Zn_x$ (x = 0.5, 1) [6] and $Zr_{65}Al_{7.5}Ni_5Cu_{17.5}Zn_5$ [7] resulted in crystallization enhancement. In this paper we explore magnetic properties and crystallization as a consequence of rapid solidification process in $Fe_{73.5-x}Zn_xCu_1Nb_3Si_{13.5}B_9$ (x = 1, 3, 5) ribbons employing melt-spinning technique.

2. Experimental

The samples in form of ribbons with chemical composition $Fe_{73.5-x}Zn_xCu_1Nb_3Si_{13.5}B_9$ (x = 1, 3, 5) were prepared by melt spinning technique. The ribbons are 2 mm wide and 50 μm thick at the linear speed of cooling rate 30 m/s. Their structure was investigated by X-ray diffraction (XRD) method. XRD measurements were performed at the BW5 beamline at DESY/HASYLAB (Hamburg, Germany). The samples were illuminated for 20 s by X-rays of wavelength 0.124 Å. XRD patterns were collected in symmetric transmission geometry using a MAR 345 two-dimensional (2D) image plate detector (2300 × 2300 pixels, 150 × 150 μm^2 pixel size), which was mounted perpendicular to the incident X-ray beam. Radiation energy was determined by fitting a standard reference LaB_6 sample. The saturation magnetization (M_S) measurements of as-quenched ribbons were performed by vibration sample magnetometer (VSM). Coercivity was determined from hysteresis loops traced with fluxmeter in quasi DC magnetic field.

3. Results and discussion

The XRD patterns of $Fe_{73.5-x}Zn_xCu_1Nb_3Si_{13.5}B_9$ (x = 1, 3, 5) as-quenched ribbons are presented in Fig. 1. The Bragg peaks in XRD pattern of $x = 5$ belong to cubic Fe_3Si phase (ICSD 412838, space group: $Fm3m$). The average grain size of Fe_3Si phase ($\approx$ 25 nm) was determined from the Debye–Scherrer equation [8]:

$$L = \frac{(0.9)\lambda}{\beta \cos\theta}\,.$$

Here, L is the coherent length, λ is the X-ray wavelength, β is the full-width at half-maximum of the XRD peak and θ is the Bragg angle. Small crystalline fraction Fe_3Si phase is detectable in $x = 3$ sample (small Bragg peaks) as well. Only the sample $x = 1$ is in a fully amorphous state as it is documented by its diffraction profile consisting of two diffuse peaks without any indications of the Bragg peaks.

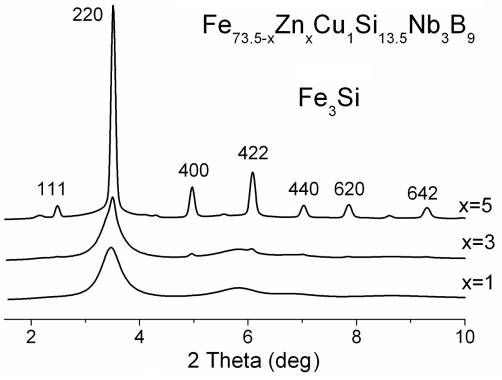

Fig. 1. XRD patterns of $Fe_{73.5-x}Zn_xCu_1Nb_3Si_{13.5}B_9$ (x = 1, 3, 5) as quenched ribbons. Indexed peaks correspond to the Bragg reflections of Fe_3Si phase.

The Fourier inversion of structural factor $S(Q)$ obtained from diffraction data gives the reduced radial dis-

tribution function

$$G(r) = \frac{2}{\pi} \int_{Q_{\min}}^{Q_{\max}} Q\,[S(Q) - 1] \sin(Qr)\,\mathrm{d}Q\,,$$

where Q is the momentum transfer. The $G(r)$ provides information about probability of finding an atom in spherical shell at a distance r from an arbitrary atom.

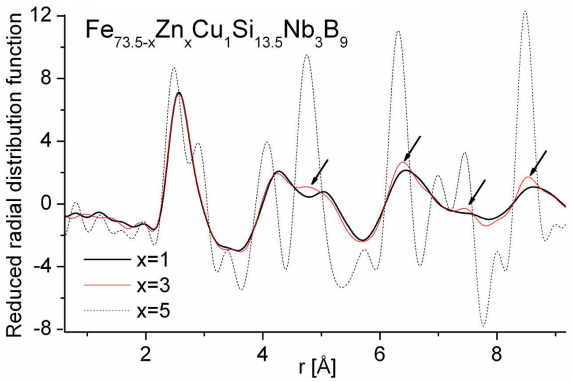

Fig. 2. Reduced radial distribution function of $Fe_{73.5-x}Zn_xCu_1Nb_3Si_{13.5}B_9$ (x = 1, 3, 5) as-quenched ribbons. Differences between $G(r)$ functions for $x = 1$ and $x = 3$ samples are marked with inclined arrows.

TABLE

Summarization of magnetic parameters for the as-quenched and annealed $Fe_{73.5-x}Cu_1Si_{13.5}B_9Nb_3Zn_x$ (x = 1, 3, 5) ribbons.

	M_s [A m^2 kg^{-1}]	H_c [A m^{-1}] (as-quenched)
$x = 1$	127.4	4.77
$x = 3$	112.8	6.8
$x = 5$	81.1	12.5

The determined $G(r)$ functions of $Fe_{73.5-x}Zn_xCu_1Nb_3Si_{13.5}B_9$ (x = 1, 3, 5) as-quenched samples are shown in Fig. 2.

With increasing degree of structural ordering amplitudes and sharpness of $G(r)$ function increase as it can be seen in Fig. 2. $G(r)_{x=5}$ shows pronounced and well defined maxima, whose positions are in good agreement with the interatomic distances in the Fe_3Si structure. On the other hand, maxima of $G(r)_{x=1}$ and $G(r)_{x=3}$ are evidently broader than those of $G(r)_{x=5}$. Additionally it is seen that main peaks (in the interval 2–3.5 Å) of $G(r)_{x=1}$ and $G(r)_{x=3}$ are very similar suggesting a similar short local ordering in both, $x = 1$ and $x = 3$ samples. Deviations from this similarity (marked with inclined arrows in Fig. 2) are clearly visible for distances r greater than 4.5 Å. These differences reflect the fact that the $x = 3$ sample contains small amount of crystalline Fe_3Si phase in the amorphous matrix compared with the fully amorphous $x = 1$ sample (Fig. 2).

The values of coercivity of as-quenched samples (Table) are apparently lower in comparison to the results of [6] ($\approx$ 26 A/m for as-quenched samples). Increasing value of coercivity with higher Zn content can be interpreted as follows: Crystallization of investigated samples (see Fig. 1, Fig. 2) is a result of rapid solidification process which leads to hinder domain wall movement (magnetocrystalline anisotropy increasing) [9], analogous to the results reported in [6]. The decrease of magnetocrystalline anisotropy (magnetic softening) can be reached by annealing process when the nanostructure is created after (or as a consequence) of structural relaxation process [10].

The decrease of M_S values (listed in Table) is caused by decreasing Fe content.

4. Conclusion

From prepared $Fe_{73.5-x}Zn_xCu_1Nb_3Si_{13.5}B_9$ (x = 1, 3, 5) as-quenched ribbons the $x = 1$ sample was in amorphous state. The $x = 3$ sample contains a small fraction of Fe_3Si phase and the sample with $x = 5$ is in nanocrystalline state with the average grain size of about 25 nm. The shape of main peaks (in the range 2–3.5 Å) of $G(r)_{x=1}$ and $G(r)_{x=3}$ indicate similar short local ordering in both, $x = 1$ and $x = 3$ samples. Increasing Zn content enhances crystallization during solidification which leads to increase of magnetocrystalline anisotropy and consequently to increasing value of coercivity.

Acknowledgments

The paper was supported by Slovak Grant Agency VEGA (1/0167/10 and 1/0311/10) and it was done in the frame of the project "Centre of Excellence of progressive materials with nano- and submicron microstructure", with support of the Operational Program Research and Development financed from European Regional Development Fund.

References

[1] Y. Yoshizava, S. Oguma, K. Yamauchi, *J. Appl. Phys.* **64**, 6044 (1988).

[2] K. Suzuki, A. Makino, A. Inoue, T. Masumoto, *J. Appl. Phys.* **70**, 6232 (1991).

[3] W. Lu, L. Yang, B. Yan, W.H. Huang, *Mater. Sci. Eng.* **128**, 179 (2006).

[4] M.A. Willard, D.E. Laughlin, M.E. McHenry, D. Thoma, K. Sickafus, J.O. Cross, V.G. Harris, *J. Appl. Phys.* **84**, 6773 (1998).

[5] G. Herzer, in: *Handbook of Magnetic Materials*, Ed. K.H.J. Buschow, Vol. 10, Amsterdam 1997, p. 415.

[6] N. Chau, N.Q. Hoa, N.D. The, L.V. Vu, *J. Magn. Magn. Mater.* **303**, 415 (2006).

[7] Ch. Li, A. Inoue, *J. Alloys Comp.* **325**, 230 (2001).

[8] R. Nowosielski, J.J. Wysocki, I. Wnuk, P. Gramatyka, *J. Mater. Process. Technol.* **175**, 324 (2006).

[9] V. Franco, C.F. Conde, A. Conde, *J. Magn. Magn. Mater.* **185**, 353 (1998).

[10] J.M. Borrego, C.F. Conde, A. Conde, *Matter. Sci. Eng.* **304**, 491 (2001).